

Novel Multiport Output Twisted String Actuator with Self-differential Mechanism: Hand Glove Application

Dunwen Wei¹, Chengguang Cui¹, Haitao Yu¹, Tao Gao¹, Chao Li², Sajjad Hussain³, Fanny Ficuciello³

Abstract—The differential mechanism can reduce the number of actuators and efficiently distribute force or power. We proposed a novel multiport output twisted string actuator (MO-TSA) with self-differential mechanism that employs a single actuator to achieve multiport outputs. The differential MO-TSA is adaptively controlled in accordance with the force differences at each output port, thus replacing the traditional differential gears and whiffletree mechanisms. Inspired by the hand muscles, we designed one hand glove using the MO-TSA, aiming to enhance the range of achievable grasp configurations. The hand glove is capable of performing various grasps with a single actuator, resulting in a lighter and simpler hand design and revolutionizing the field of twisted string actuators (TSAs) by offering a streamlined solution for achieving versatile actuation.

I. INTRODUCTION

The use of auxiliary gloves can be crucial in enhancing strength and mobility for individuals with sensory motor impairments like spinal cord injuries or strokes [1], [2]. In soft hand gloves, the actuation subsystem, responsible for generating and transferring power to the fingers, is a significant component contributing to both the weight and cost. Researchers have investigated various actuation methods, including fluidic actuators (such as pneumatic and hydraulic systems) [3], [4], cable-driven mechanisms [5], twisted strings [6], [7], and other artificial muscles [8], [9]. These explorations aim to develop lightweight and cost-effective solutions for soft hand glove designs by optimizing the actuation mechanism's efficiency and minimizing its impact on weight and cost. For example, Walsh et al.

introduced a fully soft hand assistive device utilizing pneumatic actuation [10] featuring a fully open design with the pneumatic actuator located dorsally on the hand to assist in flexion movement. As an alternative actuation method, cable-driven mechanisms utilize electric motors and cables routed along the body. This mechanism offers advantages of precise control, high bandwidth, and remote actuation, resulting in a reduced weight. Due to these advantages, the cable-driven mechanism is the second most commonly used actuation method in the design of hand assistive devices [5], [11]. Artificial muscles, such as shape memory alloy (SMA) wires, have also been employed in the design of hand assistive devices [8], [9]. Despite the advantage of a high power-to-weight ratio, the SMA actuators suffer from problems such as lower actuation bandwidth and large hysteresis.

Twisted string actuator (TSA) is an interesting development in the design of compliant actuators capable of generating high torque and translational force [12]. The TSA twists the strings co-axially along the shaft, thereby shortening their length [13] and applying assistive forces to the intended joint in the direction of cable shortening. In addition, TSAs offer silent operation and cost-effectiveness by eliminating the need for additional gearing mechanisms. Owing to these advantages, recent years have seen a surge in the use of TSAs in the design of soft assistive devices [6], [7]. For example, Silva et al. [14] proposed a soft biomimetic hand exoskeleton with TSA for hand rehabilitation and functional enhancement. Likewise, Park et al. [15] developed a 3D printed portable hand orthosis to improve grasping functionality, using TSA actuation to achieve a balance between grip aperture and strength-weight ratio. Recently, Dragusanu et al. [16] proposed the MGlove-TS, a modular TSA actuated soft glove for hand rehabilitation.

Although the above-mentioned actuation methods meet the basic requirements for driving single-joint, the complexity of intricate hand movements, compounded by the presence of three degrees of freedom (DOF) in the fingers, poses a significant challenge. The crux of the issue lies in implementing an adaptive differential mechanism that aims to reduce the number of actuators required for optimal functioning. Various differential mechanisms, such as geared differential mechanisms, pulley differential mechanisms, and whiffletree mechanisms, are commonly used in hand exoskeletons.

Differential geared mechanisms can efficiently utilize one motor to activate multiple DOFs, allowing adaptive grasping while simultaneously reducing system complexity and costs [17]. Dragusanu et al. [18] proposed a hand exoskeleton with a geared differential mechanism to couple the motion

*This work was supported by the National Natural Science Foundation of China (Grant No. 52275282), Fundamental Research Funds for the Central Universities of China (Grant No. ZYGX2021YGCX011), the program of China Scholarships Council (Grant No.202206075010), BRIEF project funded under the National Recovery and Resilience Plan (NRRP) (No. IR0000036), LeCoR-PROC project PRIN 2022 PNRR(No. P20229CSJB), TI-RED project PRIN 2022 PNRR (No.20229N5YW8), Endotheranostics European UnionERC-2023-SyG Endotheranostics (No. 101118626) and EuROBIN Horizon Europe program framework under grant agreement (No.101070596). (Corresponding authors: Dunwen Wei, Chao Li)

¹Dunwen Wei, Chengguang Cui, Haitao Yu, and Tao Gao are with the School of Mechanical and Electrical Engineering, University of Electronic Science and Technology of China, Chengdu, 611731, China. {weidunwen, 2020040906006, 201922040426, gaotao}@uestc.edu.cn

²Chao Li is with Department of Thyroid-Oral and Maxillofacial Head Neck Surgery, Sichuan Clinical Research Center for Cancer, Sichuan Cancer Hospital & Institute, Sichuan Cancer Center, Affiliated Cancer Hospital of University of Electronic Science and Technology of China, Chengdu, 610041, China. lichao@scszlly.org.cn

³Sajjad Hussain, Fanny Ficuciello are Department of Electrical Engineering and Information Technology, University of Naples Federico II, Naples, Italy. {sajjad.hussain, fanny.ficuciello}@unina.it

of adjacent fingers and preserve individual movements.

Whiffletree mechanisms utilize rigid connections as levers to achieve differential action, ensuring even transmission of applied force between connected loads. When force is applied to the system, it propagates through the central connection point, distributing the load uniformly across both endpoints. The simplicity and robustness have led to its incorporation in the design of various underactuated prostheses [19], [20]. However, a drawback of the whiffletree mechanism is its diminished efficiency when subjected to large displacements. Specifically, during rotation, the connection points generate undesirable lateral displacement and force, posing challenges in optimizing performance [21].

Pulley-based mechanisms leverage pulleys to achieve differential behavior, wherein the mechanism response varies with the applied input force. Belter et al.[22] combined pulleys with a whiffletree system, which serves to address the limitations associated with both mechanisms individually. This enables the desired displacement without the need for wider pulleys. Bajaj et al.[23] proposed a differential mechanism based on pulleys, which enables the actuation of all four fingers through a single motor.

These differential mechanisms often require supplementary components such as gears, connecting levers, or pulley mechanisms to achieve differential function. Thus, achieving the actuation of the self-differential mechanism without additional components remains a challenging undertaking.

To overcome the above limitations, this paper presents a new multiport output twisted string actuator (MO-TSA) utilizing a single motor to achieve multiple port outputs. Unlike the traditional methods of differential gears and whiffletree mechanisms, this innovation eliminates the need for complex differential mechanisms by tailoring the differential output to each port's specific requirements. The proposed mechanism has the capability to actuate multiple DOFs by simply expanding the number of outputs to match the number of DOFs thus revolutionizing the field of TSAs by offering a streamlined solution for achieving a versatile actuation.

II. PRINCIPLE OF MULTIPORT OUTPUT MO-TSA

A. Inspiration from hand muscles

The flexibility and strength of the human hand stem not only from its inherent capabilities but also from the significant contribution of arm muscles, which transmit forces to the hand digits through tendon transmission mechanism. Majority of tendons within the hand are enclosed by protective structures known as tendon sheaths and ligaments. Originating from the muscle, the knuckle tendon travels through the carpal tunnel and extends outward in a fan-like manner, reaching out to each finger shown in Fig. 1(a). This remarkable anatomical arrangement inspired the development of a novel drive scheme, wherein a rope simulates the tendons, an outer tube emulates a tendon sheath, and a TSA, when connected to a motor, mimics muscle function i.e. force generation. This innovative design results in a driving system that closely replicates the characteristics of a soft glove.

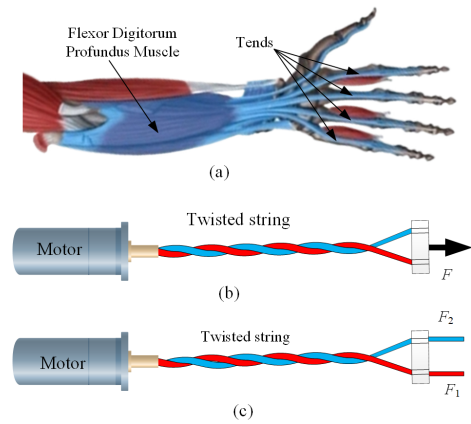


Fig. 1. Schematic diagram of multiport output twisted string actuator. (a) Hand muscle actuation. (b) Traditional TSA. (c) Multiport output TSA.

Traditional TSAs have their inherent limitations. As illustrated in Fig. 1(b), traditional TSA has only one output end to drive load. In contrast, the extrinsic muscles of the hand, specifically the flexor digitorum profundus located in the deep layer of the forearm, originate as a single muscle and split into four parts which connects to the palmar surface of the distal phalanges of the second to fifth digits, as shown in Fig. 1(a). This structure allows for independent control of these fingers. Drawing inspiration from the structure of these muscles, this research enhance existing TSAs capability by introducing multiport output of with Self-differential Mechanism. The schematic diagram of the MO-TSA is depicted in Fig. 1(c), which utilize two or more strings to drive different loads, thereby enabling the TSAs to facilitate multiple finger movements.

The MO-TSA demonstrates efficient utilization of a single motor driving multiple loads by connecting the separator's output to different loads. Structurally resembling the flexor digitorum profundus muscle in the human hand, these TSAs employ a twisted-pair of strands or multi-stranded, as the muscle and multiple single strings extended by the separator as tendons to drive finger movements. Adhering to principles of human hand motion, this design minimizes the number of motors required, reducing overall weight while ensuring robust driving capability. Additionally, these TSAs exhibit adaptive behavior, autonomously adjusting the displacement of strings when subjected to varying external loads, effectively emulating the characteristics of soft gloves when gripping objects with irregular shapes, thereby showcasing their inherent adaptive nature.

Movement adjustment occurs dynamically and adaptively by taking into consideration the variations in load size that may occur at different load ends. This adaptive feature enables the system to tailor its movement to the specific requirements of each load end, ensuring optimal performance and efficiency. In order to achieve this adaptability, the rope is constructed using multiple strands, with the exact number of strands being determined by the specific needs of the system. By composing the rope of n strands, the system can successfully accommodate the n maximum number of output

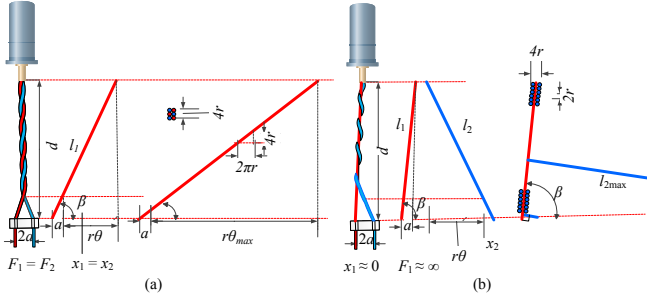


Fig. 2. Two actuation modes of MO-TSA with differential mechanism. (a) Same load force applied at both ends: $F_1 = F_2$. (b) Different loads at both ends: one output terminal is locked, resulting in the infinite force $F_1 = \infty$, while the other is free.

ports, thereby enabling the system to handle a diverse range of loads and perform at its highest capacity. This approach ensures that the movement is optimized and that the system is able to effectively meet the users' demands.

B. Model of multiport Output MO-TSA

The complexity of theoretical modeling for the MO-TSA cannot be overlooked. In addition to sharing hysteresis saturation and structural material nonlinear characteristics with traditional TSAs, the motion output also depends on load magnitude. In this section, we analysed two specific scenarios: when equal load force is applied on both sides, and when one load end is fixed. Comprehending the dynamics of the proposed multiport TSA necessitates careful consideration and implication of the following assumptions:

- Ignoring the rope deformation: We assume that no deformation of flexible material occurs during stretching and compression.
- Disregarding self-rotation influence: Assume no self-rotation generates due to the stretching force.
- without over-twisting: Despite over-twisting can introduce into the proposed multiport TSA, we assume that no over-twisting occurs during modeling.

The two special actuation modes, shown in Fig.2 are considered for this analysis. Here, the length of the torsion zone is indicated as d , the hole distance of the separator is represented by a , and the diameter of the string is indicated as r . These parameters significantly influence the kinematic characteristics of the TSA. Hence, in practical applications, adjusting these parameters through structural design allows for different transmission ratios and stiffness levels. For instance, if the length of string in the torsion zone increases as the motor shaft rotates, then the linear displacement equals the length of strings entering the torsion zone.

Case 1- Same loads at both ends: In the case of the same load force on both sides, the linear displacement can be calculated using the following equation:

$$x_1 = x_2 = x = \sqrt{d^2 + (a + r\theta)^2} - \sqrt{d^2 + a^2} \quad (1)$$

where the θ is the rotation angle of motor, and x_1 and x_2 are the linear displacement of the output terminals respectively.

The transmission ratio of TSA can be expressed as:

$$\gamma = \frac{\dot{\theta}}{\dot{x}} = \frac{\sqrt{d^2 + (a + r\theta)^2}}{r(a + r\theta)} = \frac{\cos \beta}{r} \quad (2)$$

The relation between the motor's torque T and the pulling force F is also required. Taking into account the mechanical efficiency η , the force on each side can be obtained from the force-torque equilibrium equation as follows.

$$F_1 = F_2 = \frac{F}{2} = \frac{\eta \sqrt{d^2 + (s + r\theta)^2}}{2r(s + r\theta)} T = \eta \frac{\cos \beta}{2r} T \quad (3)$$

It is pertinent to note that the MO-TSA has a limited motion range before the strings reach the point of over-twisting. This operational limit results in a compact shape of the strings, as illustrated in Fig. 2(a). From this configuration, we can determine the maximum rotation angle of motor.

$$\theta_{max} = \frac{\pi d - 2a}{2r} \quad (4)$$

The maximum linear displacement is

$$x_{max} = \sqrt{d^2 - \left(\frac{\pi d}{2}\right)^2} - \sqrt{d^2 + a^2} \quad (5)$$

Case 2- Different loads at both ends: The model complexity increases When different loads are attached to both ends. To simplify the analysis here we consider a limiting scenario as illustrated in Fig. 2(b), where one terminal is locked, and the other end side is free to move. In this configuration, the locked string remains straight, while the other string winds along it. The limit twist angle and the stretched length of string, under this configuration, can be calculated as follows.

$$x_2 = \sqrt{\left(\sqrt{d^2 + a^2} - \frac{\theta r}{\pi}\right)^2 + \frac{4\theta r a^2}{\pi \sqrt{d^2 + a^2}}} + 2r\theta - \sqrt{d^2 + a^2} \quad (6)$$

$$\theta_{max} = \frac{\pi (d^2 - a^2)}{r \sqrt{d^2 + a^2}} \quad (7)$$

$$x_{2,max} = \frac{(2\pi - 1) (d^2 - a^2)}{2\sqrt{d^2 + a^2}} \quad (8)$$

III. SOFT GLOVE WITH MULTIPOUT OUTPUT MO-TSA

Fig. 3(a) presents schematics of the proposed soft glove incorporating MO-TSA. Similar to motor cable-driven actuation mechanisms, the TSA allows for remote actuation, effectively separating the driving component from the glove body. This design feature is crucial as it prevents direct load application to the user's hand, thereby improving the users' comfort. Moreover, TSA exhibits several desirable characteristics that make it well-suited for powering bionic soft gloves. Its smooth operation ensures seamless movement, while its high efficiency contributes to energy conservation. Furthermore, its structural and functional similarity to human hand movement patterns offers distinct advantages over traditional direct motor, pneumatic, and hydraulic drives, ensuring enhanced flexibility and safety during operation.

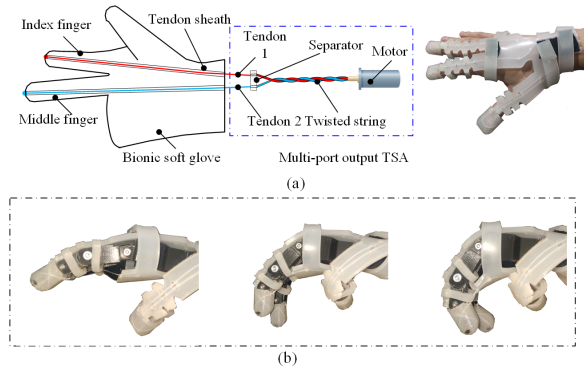


Fig. 3. Principle of the bionic soft glove with MO-TSA. (a) Actuation diagram of bionic soft glove using MO-TSA. (b) Finger movement of bionic soft gloves with MO-TSA

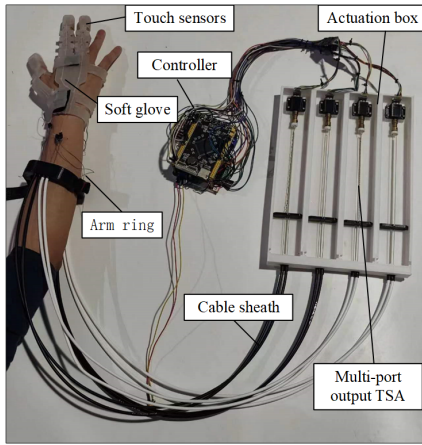


Fig. 4. Experimental platform of the bionic soft glove with MO-TSA

The TSA enables the transmission of force and torque over a considerable distance, thereby effectively separating the driving component from the glove body. This separation is crucial in order to prevent the entire load from being applied directly to the user's hand. In addition to this, the second point highlights the smooth operation, high efficiency, and low noise characteristics of the TSA. These features make it perfectly suitable for meeting the driving requirements of bionic soft gloves. Finally, the third point emphasizes the structural and functional similarity of the TSA to the movement patterns of human hands. This similarity is advantageous compared to traditional direct motor drives, pneumatic drives, and hydraulic drives, as it provides better flexibility and safety during the driving process.

In the context of finger movement, the under-actuation coupling method is employed, utilizing two tendons, palmar and dorsal, per finger to facilitate flexion and extension movements. The device incorporates four TSAs: two for supporting flexion and extension movements of the index and middle fingers, and two for supporting thumb flexion and extension. This approach parallels the principles governing the deep flexor muscle of the finger, thus driving the overall movement of the hand. As a result, this method efficiently reduces the number of actuators required, optimizing system efficiency.

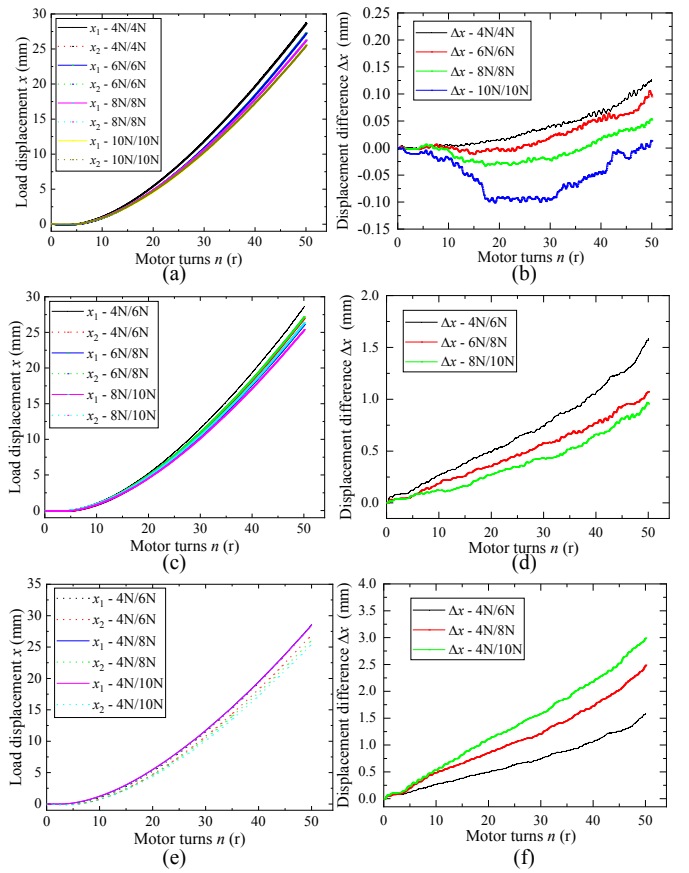


Fig. 5. Experimental results of MO-TSA. (a) Terminal displacement under the same load force. (b) Displacement difference under the same load. (c) Terminal displacement under equidifferential load. (d) Displacement difference under equidifferential load. (e) Terminal displacement under differential increasing load. (f) Displacement difference under differential increasing load.

Fig.3(b) illustrates the movement of bionic soft gloves when worn on a prosthetic hand. Fig.4 illustrates the bionic soft gloves with MO-TSA. In this diagram, it is evident that the driving tendon plays a crucial role in driving the movement of the gloves. This serves as concrete evidence that bionic soft gloves are capable of flexing and extending the fingers under dynamic drive conditions. This ability is of great significance as it allows for more natural and realistic movement of the fingers, enhancing the overall functionality and usability of the gloves.

IV. EXPERIMENTAL RESULTS

A. Experiments of MO-TSA

To examine and confirm the displacement of the two extremities of the MO-TSA under varying load conditions, a multitude of experiments were meticulously devised, and subsequent verification tests were methodically executed by incrementally adding loads of diverse weights at the respective ends. The team of researchers, in their experimental endeavors, gauged the displacement of the two load ends of the MO-TSA by systematically adding loads of 4N and 8N at each terminal.

As illustrated in Fig.5 (a), the displacement of both outputs is displayed when the load on both ends is uniform. It can be

clearly observed that the displacement-motor position curves on both ends essentially overlap, and the discrepancy in displacement is below ± 0.1 mm, signifying that when the load is equitable, the motion characteristics of the two load ends of the MO-TSA are indistinguishable shown in Fig.5 (b). Concurrently, it is noteworthy that as the load applied to both ends intensifies, the displacement at the actuator's extremity diminishes. Notwithstanding the fact that the aggregate load amplifies by 4N, the reduction in displacement gradually diminishes with the progressive augmentation of the total load. Fig.5 (c) presents a visual representation of the displacement of the two outputs in a scenario where the difference between the loads at both ends is equal and measures 2N. The graphical illustration demonstrates that the end with a smaller load exhibits a greater displacement. In addition, as the number of turns of the motor increases, there is an observable upward trend in the disparity of displacement between the two ends. Specifically, when the motor position reaches 50 turns, the discrepancy in displacement for the 4N/6N group can extend up to 1.6 mm, which represents approximately 6% of the total displacement length. Moreover, it should be noted from Fig.5(d) that as the overall load on both ends escalates, the impact of the displacement difference and the unit load difference between the two ends on the displacement difference gradually diminishes. Therefore, the influence of these factors on the disparity in displacement gradually subsides as the load increases. Fig.5 (e) illustrates the displacement of the two outputs as the load discrepancy between the two ends gradually increases. In other words, when one end bears a fixed load of 4N, 6N, 8N, and 10N loads are successively applied to the other end. Upon careful observation, it becomes evident that there exists a positive correlation between the load difference and the displacement difference between the two ends. Moreover, the displacement distance at the 4N end remains almost unaltered. Nevertheless, as the total load on both ends increased, the degree of change in displacement difference diminishes with each subsequent increase in unit load Fig.5 (f).

Upon analyzing the empirical findings, it is evident that a TSA with multiport output has the capability to simultaneously drive two or more load ends. As the string spirals during twisting, differing loads on each end induces different deformations, resulting in an uneven displacement of the two ends. This particular characteristic, when implemented in bionic soft gloves, proves to be highly advantageous. For instance, when one finger initially makes contact with an object, the object's reaction force on the fingertip triggers a rapid increase in string tension. During this period, it is essential to ensure that the displacement of this particular end does not persistently rise, thereby allowing the twisting process to continue for a specific duration until the other finger also makes contact with the object. At this juncture, the twisting process either halts or the string reaches its limit. Integration of this feature into soft bionic glove allows not only to control all the fingers with one motor, but also allows for adaptive grasping without using any external differential mechanism, thereby reducing the overall weight and cost

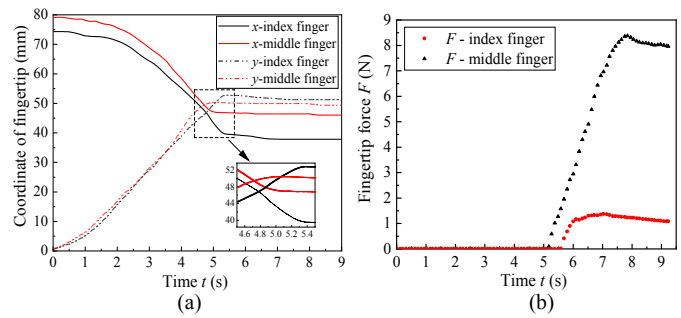


Fig. 6. Fingertip motion trajectory of adaptively grasping object using the soft hand glove with MO-TSA. (a) Fingertip motion trajectory. (b) Fingertip force.

of the device.

B. Experiments of soft glove

To evaluate the motion characteristics and performance of MO-TSA in the bionic soft glove in Fig.4, we conducted an experiment of grasping a single object. The main objective was to examine the adaptive behavior of the proposed TSA, when subjected to different loads. In this experiment, two loads were applied to the front and back along the path of motion of the two fingers, simulating the scenario in which the fingers touch an object sequentially. The internal movement of the index finger and the middle finger was independently controlled using the two output terminals of a MO-TSA. To proceed with the experiment, initially both the fingers were devoid of any load to observe their initial movement state.

The trajectory of fingertip movement was analyzed when actuated by the MO-TSA. It was observed that at the beginning of the motion, when the bionic soft gloves were in motion without any load, the movement of the index finger and middle finger was synchronized, as both ends of the strings were in the same position. However, as the movement continued, the load position of the middle finger shifted to the front, resulting in the middle finger making contact with the object before the index finger. Consequently, the movement of the middle finger was constrained and its position remained unchanged. Meanwhile, the twisting process continued, leading to a rapid increase in the force of the middle finger fingertip, as depicted in Fig.6. Interestingly, despite the middle finger making contact with the object, the index finger was still in the process of moving towards it. This observation demonstrates the adaptive characteristics of the MO-TSA, as it allowed the index finger to continue its movement until it also made contact with the object.

To provide further context, it is worth mentioning the work of Smaby et al.[24], who conducted a study on fingertip force during various daily life activities. They found that activities such as plugging in power plugs and grabbing objects typically require fingertips to exert force about 20N. Comparing this finding to Fig.6(b), where it is evident that the fingertip strength of the middle finger can reach 8N, it becomes apparent that this level of force can provide approximately 40% of the fingertip force required for normal human hands to actively engage in grip rehabilitation training. These

results underscore the potential of the MO-TSA in facilitating gripping actions when integrated with bionic soft gloves.

In conclusion, the multiport output capture experiment successfully shed light on the motion characteristics of the MO-TSA on bionic soft gloves. The experiment involved simulating the gripping movement of two fingers and analyzing their movement trajectories. The findings showcased the adaptability of the MO-TSA, as well as its potential to provide a significant portion of the fingertip force required for grip rehabilitation training. This research contributes to the understanding and development of bionic soft gloves, paving the way for advancements in prosthetic technology.

V. CONCLUSION AND FUTURE WORK

Based on the anatomical structure of the flexor digitorum profundus muscle, a novel MO-TSA was designed specifically to address the differential mechanism requirements of bionic soft gloves. Experimental analysis was conducted to investigate the motion characteristics of MO-TSA to validate its effectiveness. The results demonstrated that the MO-TSA has the remarkable ability to adaptively alter the displacement characteristics of the end based on the varying loads experienced at both ends. In addition, a prototype was successfully constructed to illustrate the fundamental principles of bionic soft gloves. The findings not only confirmed the self-differential mechanism of MO-TSA, but also provided substantial evidence that they can adaptively execute the grasping tasks. Looking ahead, future research endeavors will focus on high accuracy modeling and control methods, specifically targeting differential operating under different loads. The ultimate objective of these studies is to further enhance overall performance.

REFERENCES

- [1] K. Anandan, N. Rajagopalan, Mohanavelu, and S. Mary, "Design and development of biosignal controlled hand exoskeleton for assistive purposes," *Journal of Mechanics in Medicine and Biology*, p. 2340033, 2023.
- [2] T. Bagneschi, D. Chiaradia, G. Righi, G. Del Popolo, A. Frisoli, and D. Leonardis, "a soft hand exoskeleton with a novel tendon layout to improve stable wearing in grasping assistance," *IEEE Transactions on Haptics*, vol. 16, no. 2, pp. 311–321, 2023.
- [3] D. Hu, J. Zhang, Y. Yang, Q. Li, D. Li, and J. Hong, "A novel soft robotic glove with positive-negative pneumatic actuator for hand rehabilitation," in *2020 IEEE/ASME International Conference on Advanced Intelligent Mechatronics (AIM)*. IEEE, 2020, pp. 1840–1847.
- [4] X. Cao, K. Ma, Z. Jiang, and F. Xu, "A soft robotic glove for hand rehabilitation using pneumatic actuators with jamming structure," in *2021 40th Chinese Control Conference (CCC)*. IEEE, 2021, pp. 4120–4125.
- [5] D. Xu, Q. Wu, and Y. Zhu, "Development of a soft cable-driven hand exoskeleton for assisted rehabilitation training," *Industrial Robot: the international journal of robotics research and application*, vol. 48, no. 2, pp. 189–198, 2021.
- [6] T. Tsabedze, E. Hartman, C. Brennan, and J. Zhang, "A compliant robotic wrist orthosis driven by twisted string actuators," in *2021 International Symposium on Medical Robotics (ISMR)*, Nov. 2021, pp. 1–7.
- [7] F. Li, J. Chen, Z. Zhou, J. Xie, Z. Gao, Y. Xiao, P. Dai, C. Xu, X. Wang, and Y. Zhou, "Lightweight soft robotic glove with whole-hand finger motion tracking for hand rehabilitation in virtual reality," *Biomimetics*, vol. 8, no. 5, p. 425, 2023.
- [8] A. Villoslada, C. Rivera, N. Escudero, F. Martin, D. Blanco, and L. Moreno, "Hand exo-muscular system for assisting astronauts during extravehicular activities," *Soft robotics*, vol. 6, no. 1, pp. 21–37, 2019.
- [9] R. Srivastava, M. Singh, G. D. Gomes, N. Murray, and D. Devine, "Sm-exo: Shape memory alloy-based hand exoskeleton for cobotic application," in *2022 31st IEEE International Conference on Robot and Human Interactive Communication (RO-MAN)*. IEEE, 2022, pp. 1277–1284.
- [10] P. Polygerinos, S. Lyne, Z. Wang, L. F. Nicolini, B. Mosadegh, G. M. Whitesides, and C. J. Walsh, "Towards a soft pneumatic glove for hand rehabilitation," in *2013 IEEE/RSJ International Conference on Intelligent Robots and Systems*, 2013, pp. 1512–1517.
- [11] R. C. Silva, B. G. Lourenço, P. H. Ulhoa, E. A. Dias, F. L. da Cunha, C. P. Tonetto, L. G. Villani, C. B. Vimieiro, G. A. Lepski, M. Monjardim, *et al.*, "Biomimetic design of a tendon-driven myoelectric soft hand exoskeleton for upper-limb rehabilitation," *Biomimetics*, vol. 8, no. 3, p. 317, 2023.
- [12] J. Zhang, J. Sheng, C. T. O'Neill, C. J. Walsh, R. J. Wood, J.-H. Ryu, J. P. Desai, and M. C. Yip, "Robotic artificial muscles: Current progress and future perspectives," *IEEE Transactions on Robotics*, vol. 35, no. 3, pp. 761–781, 2019.
- [13] I. Gaponov, D. Popov, and J.-H. Ryu, "Twisted string actuation systems: A study of the mathematical model and a comparison of twisted strings," *IEEE/ASME Transactions on mechatronics*, vol. 19, no. 4, pp. 1331–1342, 2013.
- [14] R. C. Silva, B. G. Lourenço, P. H. Ulhoa, E. A. Dias, F. L. da Cunha, C. P. Tonetto, L. G. Villani, C. B. Vimieiro, G. A. Lepski, and M. Monjardim, "Biomimetic design of a tendon-driven myoelectric soft hand exoskeleton for upper-limb rehabilitation," *Biomimetics*, vol. 8, no. 3, p. 317, 2023.
- [15] C. B. Park and H.-S. Park, "Portable 3d-printed hand orthosis with spatial stiffness distribution personalized for assisting grasping in daily living," *Frontiers in Bioengineering and Biotechnology*, vol. 11, p. 895745, 2023.
- [16] M. Dragusanu, D. Troisi, B. Suthar, I. Hussain, D. Prattichizzo, and M. Malvezzi, "Mglove-ts: A modular soft glove based on twisted string actuators and flexible structures," *Mechatronics*, vol. 98, p. 103141, apr 2024.
- [17] T. Tamamoto, K. Takeuchi, and K. Koganezawa, "Development of gripper to achieve envelope grasping with underactuated mechanism using differential gear," *Journal of Robotics and Mechatronics*, vol. 30, no. 6, pp. 855–862, 2018.
- [18] M. Dragusanu, D. Troisi, A. Villani, D. Prattichizzo, and M. Malvezzi, "Design and prototyping of an underactuated hand exoskeleton with fingers coupled by a gear-based differential," *Frontiers in Robotics and AI*, vol. 9, p. 862340, 2022.
- [19] B. Busby, G. Gao, and M. Liarokapis, "An adaptive, lightweight, body-powered system for prosthetic hands equipped with a selectively lockable differential mechanism," in *2023 45th Annual International Conference of the IEEE Engineering in Medicine & Biology Society (EMBC)*. IEEE, 2023, pp. 1–7.
- [20] G. P. Kontoudis, M. V. Liarokapis, A. G. Zisimatos, C. I. Mavrogianis, and K. J. Kyriakopoulos, "Open-source, anthropomorphic, underactuated robot hands with a selectively lockable differential mechanism: Towards affordable prostheses," in *2015 IEEE/RSJ international conference on intelligent robots and systems (IROS)*. IEEE, 2015, pp. 5857–5862.
- [21] L. Gerez, J. Chen, and M. Liarokapis, "On the development of adaptive, tendon-driven, wearable exo-gloves for grasping capabilities enhancement," *IEEE Robotics and Automation letters*, vol. 4, no. 2, pp. 422–429, 2019.
- [22] J. T. Belter and A. M. Dollar, "Novel differential mechanism enabling two dof from a single actuator: Application to a prosthetic hand," in *2013 IEEE 13th International Conference on Rehabilitation Robotics (ICORR)*. Seattle, WA: IEEE, June 2013, pp. 1–6.
- [23] A. Bajaj, V. Jain, P. Kumar, A. Unal, and A. Saxena, "Soft hand exoskeleton for adaptive grasping using a compact differential mechanism," in *Mechanism and Machine Science*, D. Sen, S. Mohan, and G. K. Ananthasuresh, Eds. Singapore: Springer Singapore, 2021, pp. 733–746.
- [24] N. Smaby, E. Johanson, B. Baker, D. E. Kenney, W. M. Murray, and V. R. Hentz, "Identification of key pinch forces required to complete functional tasks," *Journal of Rehabilitation Research & Development*, vol. 41, no. 2, 2004.